

Adaptive Non-myopic Quantizer Design for Target Tracking in Wireless Sensor Networks

Sijia Liu*, Engin Masazade†, Xiaojing Shen‡, Pramod K. Varshney*

*Syracuse University, NY, 13244, USA, {sliu17, varshney}@syr.edu

† Yeditepe University, Istanbul, 34755, Turkey, engin.masazade@yeditepe.edu.tr

‡ Sichuan University, Chengdu, 610064, China, shenxj@scu.edu.cn

Abstract—In this paper, we investigate the problem of non-myopic (multi-step ahead) quantizer design for target tracking using a wireless sensor network. Adopting the alternative conditional posterior Cramér-Rao lower bound (A-CPCRLB) as the optimization metric, we theoretically show that this problem can be temporally decomposed over a certain time window. Based on sequential Monte-Carlo methods for tracking, i.e., particle filters, we design the local quantizer adaptively by solving a particle-based non-linear optimization problem which is well suited for the use of interior-point algorithm and easily embedded in the filtering process. Simulation results are provided to illustrate the effectiveness of our proposed approach.

I. INTRODUCTION

Wireless sensor networks (WSNs), consisting of a large number of spatially distributed sensors, have been used in a wide range of promising applications such as battlefield surveillance, environment and health monitoring. However, due to the limited communication and energy resources, it is desirable that only quantized data be transmitted from local sensors to the fusion center (FC).

Quantizer design for target tracking has been recently studied in the literature [1]–[4]. In [1], the authors employed a static quantizer, first proposed in [5], to track a moving target, where the optimal quantization thresholds are determined by maximizing the Fisher information about the signal amplitude contained in quantized data. Although this approach is robust and requires minimum prior information about the system, it doesn't yield the optimal solution for tracking scenarios where the target state is random and dynamic. An adaptive binary quantizer and uniform quantizer are proposed in [2] and [3], respectively, where the local quantizers are designed at FC for every time step. In [4], a more general framework for designing adaptive identical/non-identical quantizers is presented where the trace of the direct conditional posterior Cramér-Rao lower bound (D-CPCRLB [6]) is minimized. However, D-CPCRLB yields an intractable objective function, which leads to a high computational complexity in optimization. Therefore, to satisfy the real-time operational requirement of the adaptive system, it is essential to seek a tractable objective function and develop an efficient algorithm for quantizer design.

Fisher information matrix (FIM) has been used in [1], [3]–[5] as the performance metric, where the mean square error (MSE) is lower bounded by the inverse of FIM. However, the FIM is generally a matrix. It is important to use a suitable scalar norm of it to obtain a quantity related to the information

content. Authors in [4] employ the trace of the inverse of FIM. The determinant of FIM is used in [1], which is inversely proportional to the volume of the uncertainty ellipsoid. In this work, we adopt the trace of FIM as the performance criterion and will theoretically show that maximizing the trace of FIM does not lose the optimality of maximizing FIM in the sense of positive semidefinite cone [7], [8]. Since the trace operator is linear, we can also show that the trace of FIM yields a tractable objective function for optimization.

For adaptive quantizers proposed in [2]–[4], we note that FC is required to feed back the quantization thresholds to local sensors at every time step (a.k.a., the *myopic/greedy* design strategy [9]). However, continual transmissions might result in data collisions and channel congestion. In order to reduce the amount of communication, we design adaptive quantizers using the *non-myopic* (i.e., multi-steps ahead) strategy, which has drawn recent attention in resource management, e.g., [1], [9], [10]. In general, myopic design has lower computational complexity than the non-myopic case [9]. However, we will show that the non-myopic quantizer design can be temporally decomposed based on the alternative conditional posterior Cramér-Rao lower bound (A-CPCRLB [6]), which, unlike D-CPCRLB used in [4], yields a recursive form of the information matrix. With the aid of particle filtering methods [12], the problem of non-myopic quantizer design is expressed as a non-linear optimization problem which is easily solved by the interior-point algorithm.

II. PROBLEM FORMULATION

In this paper, the task of the WSN is to monitor a single target moving in a two-dimensional Cartesian coordinate plane. At sampling time t , the target state is defined by a 4×1 dimensional vector $\mathbf{x}_t = [x_t, y_t, \dot{x}_t, \dot{y}_t]$ where (x_t, y_t) and (\dot{x}_t, \dot{y}_t) denote the target location and velocity in the 2D plane, respectively. The target state evolves according to

$$\mathbf{x}_{t+1} = F\mathbf{x}_t + \mathbf{w}_t, \quad (1)$$

where $\mathbf{w}_t \sim \mathcal{N}(\mathbf{0}, Q)$, the state transition matrix F and the process noise covariance Q are given by [1]

$$F = \begin{bmatrix} 1 & 0 & \Delta & 0 \\ 0 & 1 & 0 & \Delta \\ 0 & 0 & 1 & 0 \\ 0 & 0 & 0 & 1 \end{bmatrix} \quad Q = q \begin{bmatrix} \frac{\Delta^3}{3} & 0 & \frac{\Delta^2}{2} & 0 \\ 0 & \frac{\Delta^3}{3} & 0 & \frac{\Delta^2}{2} \\ \frac{\Delta^2}{2} & 0 & \Delta & 0 \\ 0 & \frac{\Delta^2}{2} & 0 & \Delta \end{bmatrix}. \quad (2)$$

In (2), Δ and q denote the sampling interval between adjacent sensor measurements and the process noise parameter, respectively.

We further consider N sensors deployed in a region of interest (ROI) and each of them reports a noisy measurement in the form of signal power [1], [4]

$$y_t^i = h_t^i(\mathbf{x}_t) + v_t^i, \quad h_t^i(\mathbf{x}_t) = \sqrt{\frac{P_0}{1+(d_t^i)^2}} \quad (3)$$

for $i = 1, 2, \dots, N$, where $v_t^i \sim \mathcal{N}(0, \sigma_v^2)$, P_0 denotes the signal power of the source, d_t^i is the distance between the target and the i th sensor, $d_t^i = \sqrt{(x_i - x_t)^2 + (y_i - y_t)^2}$, where (x_i, y_i) is the position of the i th sensor in the 2D plane.

Each sensor quantizes its measurement to M bits as given below

$$u_t^i = \begin{cases} 0 & -\infty < y_t^i \leq \gamma_{t,1}^i \\ \vdots & \vdots \\ L-1 & \gamma_{t,L-1}^i < y_t^i < +\infty \end{cases}, \quad (4)$$

where u_t^i denotes the quantized measurement of the i th sensor at time step t , $L = 2^M$, and the vector $\gamma_t^i := [\gamma_{t,1}^i, \dots, \gamma_{t,L-1}^i]^T$ corresponds to the quantization strategy of sensor i . For notational consistency, let $\gamma_{t,0}^i = -\infty$ and $\gamma_{t,L}^i = \infty$. It is clear from (4) that the probability of a particular quantization output l is

$$p(u_t^i = l | \mathbf{x}_t) = Q\left(\frac{\gamma_{t,l}^i - h_t^i(\mathbf{x}_t)}{\sigma_v}\right) - Q\left(\frac{\gamma_{t,l+1}^i - h_t^i(\mathbf{x}_t)}{\sigma_v}\right), \quad (5)$$

where $Q(\cdot)$ is the complementary distribution function of the standard Gaussian distribution. Under the assumption of conditionally independent observations at local sensors, the observation likelihood function at time t can be written as

$$p(\mathbf{u}_t | \mathbf{x}_t) = \prod_{i=1}^N p(u_t^i | \mathbf{x}_t), \quad (6)$$

where $\mathbf{u}_t = [u_t^1, u_t^2, \dots, u_t^N]^T$ denotes the collection of quantized measurements from N sensors.

A. Alternative conditional posterior Cramér-Rao lower bound (A-CPCRLB)

A conditional posterior Cramér-Rao lower bound (C-PCRLB) is proposed in [11] by incorporating the history of actual sensor observations, which can provide a tighter error bound than the conventional PCRLB. Nevertheless, obtaining C-PCRLB is not computationally efficient due to the presence of the auxiliary Fisher information matrix [11, Thm. 1]. Therefore, Zheng *et al.* in [6] presented an alternative conditional PCRLB (A-CPCRLB), which is direct and more compact. In this work, we adopt A-CPCRLB as the performance criterion for quantizer design.

Let $\mathbf{x}_{0:t}$ and $\mathbf{u}_{1:t}$ denote the state vector and measurements up to time t . Then the conditional mean squared error of the state vector $\mathbf{x}_{0:t}$ is lower bounded by the inverse of the conditional Fisher information matrix (C-FIM) as in [11]

$$E\{[\hat{\mathbf{x}}_{0:t+1} - \mathbf{x}_{0:t+1}][\hat{\mathbf{x}}_{0:t+1} - \mathbf{x}_{0:t+1}]^T | \mathbf{u}_{1:t}\} \geq J^{-1}(\mathbf{x}_{0:t+1} | \mathbf{u}_{1:t}).$$

Let $J(\mathbf{x}_{t+1} | \mathbf{u}_{1:t})$ be the matrix whose inverse equals the lower-right corner submatrix of $J^{-1}(\mathbf{x}_{0:t+1} | \mathbf{u}_{1:t})$. Then the matrix $J(\mathbf{x}_{t+1} | \mathbf{u}_{1:t})$ provides a lower bound on the mean square error (MSE) of estimating \mathbf{x}_{t+1} . As shown in [6, Corollary 1], for the linear Gaussian model (1), the C-FIM $J(\mathbf{x}_{t+1} | \mathbf{u}_{1:t})$ can be computed as follows,

$$J_{t+1} \approx (Q + F J_t^{-1} F^T)^{-1} + E_{p_{t+1}^c} \{-\nabla_{\mathbf{x}_{t+1}}^{\mathbf{x}_{t+1}} \ln p(\mathbf{u}_{t+1} | \mathbf{x}_{t+1})\}, \quad (7)$$

where for notational simplicity we use J_{t+1} instead of $J(\mathbf{x}_{t+1} | \mathbf{u}_{1:t})$, $\nabla_{\mathbf{x}}^{\mathbf{x}}$ is the second-order partial derivative with respect to \mathbf{x} and $p_{t+1}^c \triangleq p(\mathbf{x}_{t+1}, \mathbf{u}_{t+1} | \mathbf{u}_{1:t})$. Note that the first term in (7) is the prediction of J_t using the state evolution model and the second term indicates the information based on the updated measurements \mathbf{u}_{t+1} at time $t+1$.

B. Non-myopic quantizer design

For the non-myopic quantizer design, we seek optimal quantizers defined in (4) over the next T_w time steps, $t+1 : t+T_w$, at time instant t . It is clear from (6) and (7) that the value of C-FIM $J_{t+\eta}$ relies on quantization thresholds of local sensors at time $t+\eta$ (denoted by $\gamma_{t+\eta} \triangleq [\gamma_{t+\eta}^1, \dots, \gamma_{t+\eta}^N]$), the previous C-FIM $J_{t+\eta-1}$, and the conditional distribution $p_{t+\eta}^c$, i.e., $p(\mathbf{x}_{t+\eta}, \mathbf{u}_{t+\eta} | \mathbf{u}_{1:t+\eta-1})$, where $\eta \in \{1, 2, \dots, T_w\}$ and J_t is used as prior information. However, during the design window $t+1 : t+T_w$, the conditional PDF $p_{t+\eta}^c$ cannot be obtained exactly for $\eta > 1$ since the quantized measurements $\mathbf{u}_{t:t+\eta-1}$ are not available at time t . Therefore, as in [10], the conditional PDF $p_{t+\eta}^c$ is approximated by its prediction $p(\mathbf{x}_{t+\eta}, \mathbf{u}_{t+\eta} | \mathbf{u}_{1:t})$, which is easily obtained using a particle filter (see more details in Sec. III).

To determine optimal thresholds $\{\gamma_{t+\eta}\}_{\eta=1, \dots, T_w}$ for the next T_w time steps, we pose the optimization problem as given below where we maximize C-FIM at time $t+T_w$,

$$\begin{aligned} & \underset{\{\gamma_{t+\eta}\}}{\text{maximize}} && J_{t+T_w}(\gamma_{t+1}, \dots, \gamma_{t+T_w}) \\ & \text{subject to} && \gamma_{t+\eta,1}^i < \dots < \gamma_{t+\eta,L-1}^i \\ & && \eta = 1, \dots, T_w \text{ and } i = 1, \dots, N \end{aligned} \quad (8)$$

where for notational simplicity we use $\{\cdot\}$ instead of $\{\cdot\}_{\eta=1, \dots, T_w}$, $\gamma_{t+\eta}$ is a $(L-1) \times N$ quantizer threshold matrix whose element $\gamma_{t+\eta,l}^i$ represents the l th threshold of sensor i at time $t+\eta$, L indicates the number of quantization levels, N is the number of sensors and T_w is the length of time window.

Note that problem (8) is a matrix optimization problem which is defined in the positive semidefinite cone [7]. Namely, if $\{\gamma_{t+\eta}^*\}$ is an optimal solution, then for an arbitrary feasible solution $\{\gamma_{t+\eta}\}$, $J_{t+T_w}(\{\gamma_{t+\eta}^*\}) \succeq J_{t+T_w}(\{\gamma_{t+\eta}\})^1$, i.e., the matrix $J_{t+T_w}(\{\gamma_{t+\eta}^*\}) - J_{t+T_w}(\{\gamma_{t+\eta}\})$ is positive semidefinite.

Furthermore, the following Proposition shows that the problem (8) can be equivalently transformed to T_w sub-problems. Each of the subproblems has a scalar objective function in terms of the trace of the Fisher information matrix with respect to the updated measurements.

¹A positive/negative semidefinite matrix A is denoted by $A \succeq 0$ or $A \preceq 0$.

Proposition 1: If problem (8) has an optimal solution, then the solution of (8) can be equivalently transformed to the solution of T_w subproblems, i.e.,

$$\begin{aligned} & \underset{\gamma_{t+\eta}}{\text{maximize}} \quad \text{tr} \left(E_{p_{t+\eta}} \left\{ -\nabla_{\mathbf{x}_{t+\eta}}^{\mathbf{x}_{t+\eta}} \ln p(\mathbf{u}_{t+\eta} | \mathbf{x}_{t+\eta}) \right\} \right) \\ & \text{subject to} \quad \gamma_{t+\eta,1}^i < \dots < \gamma_{t+\eta,L-1}^i, \quad i = 1, \dots, N \end{aligned} \quad (9)$$

for $\eta = 1, 2, \dots, T_w$, where $\text{tr}(\cdot)$ denotes the trace operator and $p_{t+\eta}^c \approx p(\mathbf{x}_{t+\eta}, \mathbf{u}_{t+\eta} | \mathbf{u}_{1:t})$.

Proof: See appendix. ■

III. PARTICLE-BASED NON-MYOPIC QUANTIZER DESIGN

In this section, we will show that the problem (9) can be further expressed in a closed form and solved efficiently with the aid of a particle filtering method.

At time step $t + \eta$, by substituting (6) into (9), the objective function in (9) can be written as

$$\sum_{i=1}^N \text{tr} \left(E_{p(\mathbf{x}_{t+\eta}, \mathbf{u}_{t+\eta}^i | \mathbf{u}_{1:t})} \left\{ -\nabla_{\mathbf{x}_{t+\eta}}^{\mathbf{x}_{t+\eta}} \ln p(u_{t+\eta}^i | \mathbf{x}_{t+\eta}) \right\} \right),$$

which indicates that seeking the optimal quantizers of N sensors at time $t + \eta$ can be obtained by equivalently solving a sequence of sub-problems, i.e.,

$$\begin{aligned} & \underset{\gamma_{t+\eta}^i}{\text{maximize}} \quad \psi(\gamma_{t+\eta}^i) \triangleq \text{tr} \left(E \left\{ -\nabla_{\mathbf{x}_{t+\eta}}^{\mathbf{x}_{t+\eta}} \ln p(u_{t+\eta}^i | \mathbf{x}_{t+\eta}) \right\} \right) \\ & \text{subject to} \quad \gamma_{t+\eta,1}^i < \dots < \gamma_{t+\eta,L-1}^i, \end{aligned} \quad (10)$$

for $i = 1, 2, \dots, N$.

Using the fact that $u_{t+\eta}^i$, $\mathbf{x}_{t+\eta}$ and $\mathbf{u}_{1:t}$ form a Markov chain and the identity for standard Fisher information matrix [13]

$$E \left[\frac{\partial \ln p(u_{t+\eta}^i | \mathbf{x}_t)}{\partial \mathbf{x}_{t,r}} \frac{\partial \ln p(u_{t+\eta}^i | \mathbf{x}_t)}{\partial \mathbf{x}_{t,j}} \right] = -E \left[\frac{\partial^2 \ln p(u_{t+\eta}^i | \mathbf{x}_t)}{\partial \mathbf{x}_{t,r} \partial \mathbf{x}_{t,j}} \right] \quad (11)$$

where $\mathbf{x}_{t,r}$ and $\mathbf{x}_{t,j}$ denote the r th entry and j th entry of state vector \mathbf{x}_t , the objective function $\psi(\gamma_{t+\eta}^i)$ in (10) can be written as

$$\psi(\gamma_{t+\eta}^i) = \sum_{r=1}^4 E_{p(\mathbf{x}_{t+\eta} | \mathbf{u}_{1:t})} \left\{ E_{p(u_{t+\eta}^i | \mathbf{x}_{t+\eta})} \left[\left(\frac{\partial \ln p(u_{t+\eta}^i | \mathbf{x}_{t+\eta})}{\partial x_{t+\eta,r}} \right)^2 \right] \right\} \quad (12)$$

where the likelihood $p(u_{t+\eta}^i | \mathbf{x}_{t+\eta})$ is given by (5).

We employ a particle based method to compute the posterior PDF. In a SIR filter [12], the posterior PDF $p(\mathbf{x}_t | \mathbf{u}_{1:t})$ is approximated by a set of particles $\{\mathbf{x}_t^s; s = 1, \dots, N_s\}$ with equal weights $1/N_s$ after the re-sampling process, where N_s is the total number of particles. Thus, the predicted PDF $p(\mathbf{x}_{t+\eta} | \mathbf{u}_{1:t})$ in (12) can be obtained by propagating particles \mathbf{x}_t^s after η steps using the state model (1). Then,

$$p(\mathbf{x}_{t+\eta} | \mathbf{u}_{1:t}) \approx \frac{1}{N_s} \sum_{s=1}^{N_s} \delta(\mathbf{x}_{t+\eta} - \mathbf{x}_{t+\eta}^s). \quad (13)$$

Substituting (5) and (13) into (12), the optimization problem (10) can be written as

$$\begin{aligned} & \underset{\gamma_{t+\eta}^i}{\text{maximize}} \quad \psi(\gamma_{t+\eta}^i) = \sum_{l=0}^{L-1} f(\gamma_{t+\eta,l}^i, \gamma_{t+\eta,l+1}^i), \\ & \text{subject to} \quad \gamma_{t+\eta,1}^i < \gamma_{t+\eta,2}^i < \dots < \gamma_{t+\eta,L-1}^i \end{aligned} \quad (14)$$

where

$$f(\gamma_{t+\eta,l}^i, \gamma_{t+\eta,l+1}^i) = \frac{1}{N_s \sigma_v^2} \sum_{s=1}^{N_s} \sum_{r=1}^4 g(\gamma_{t+\eta,l}^i, \gamma_{t+\eta,l+1}^i, \mathbf{x}_{t+\eta}^s, r),$$

and

$$\begin{aligned} & g(\gamma_{t+\eta,l}^i, \gamma_{t+\eta,l+1}^i, \mathbf{x}_{t+\eta}^s, r) \\ &= \frac{\left(\frac{\partial h_{t+\eta}^i(\mathbf{x}_{t+\eta}^s)}{\partial \mathbf{x}_{t+\eta,r}} \right)^2 \left[q\left(\frac{\gamma_{t+\eta,l}^i - b_{t+\eta}^{i,s}}{\sigma_v}\right) - q\left(\frac{\gamma_{t+\eta,l+1}^i - b_{t+\eta}^{i,s}}{\sigma_v}\right) \right]^2}{Q\left(\frac{\gamma_{t+\eta,l}^i - b_{t+\eta}^{i,s}}{\sigma_v}\right) - Q\left(\frac{\gamma_{t+\eta,l+1}^i - b_{t+\eta}^{i,s}}{\sigma_v}\right)} \end{aligned} \quad (15)$$

with $b_{t+\eta}^{i,s} \triangleq h_{t+\eta}^i(\mathbf{x}_{t+\eta}^s)$.

It is clear from (15) that the objective function of (14) is non-linear but differentiable. Therefore, the interior-point algorithm [7] is a well-suited optimization tool for solving problem (14). The procedure for non-myopic quantizer design under the SIR filtering framework is summarized in Algorithm 1.

Remark 1: It can be seen from (14) that the complexity of the non-myopic quantizer design depends on the number of Monte-Carlo particles (i.e., N_s). Fewer number of particles would reduce the computation cost but result in worse estimation performance due to the low accuracy of approximating the predicted PDF in (13). Therefore, it is important to investigate the tradeoff between the number of particles and the estimation performance.

Algorithm 1 Adaptive non-myopic quantizer design

- 1: At time t , begin with the updated particles \mathbf{x}_t^s and weights $w_t^s = N_s^{-1}$
 - 2: **for** $\eta = 1, \dots, T_w$ **do**
 - 3: Propagate particles by $\mathbf{x}_{t+1}^s = F\mathbf{x}_t^s + w_t$
 - 4: $p(x_{n+1} | u_{1:n-}) = \frac{1}{N_s} \sum_{s=1}^{N_s} \delta(x_{n+1} - x_{n+1}^s)$
 - 5: Obtain optimal thresholds γ_{t+1}^i for N sensors by solving (14) for $i = 1, \dots, N$.
 - 6: **end for**
 - 7: Feed $\{\gamma_{t+\eta}^i\}_{\eta=1, \dots, T_w}$ back to local sensors and update particles by using the corresponding quantized measurement at $t + 1, \dots, t + T_w$.
-

A. Binary Quantizers

For a binary quantizer, i.e., $L = 2$, the optimization problem (14) becomes *unconstrained*, i.e.,

$$\underset{\gamma_{t+\eta,1}^i}{\text{maximize}} \quad f(-\infty, \gamma_{t+\eta,1}^i) + f(\gamma_{t+\eta,1}^i, \infty), \quad (16)$$

whose optimality condition is presented by the following proposition.

Proposition 2: The optimality condition for the binary quantizer of sensor i at time $t + \eta$ can be expressed by a nonlinear equation

$$\begin{aligned} & \sum_{r=1}^4 \sum_{s=1}^{N_s} \left[\frac{\partial h_{t+\eta}^i(\mathbf{x}_{t+\eta}^s)}{\partial \mathbf{x}_{t+\eta,r}} \right]^2 \frac{2(\gamma_{t+\eta,1}^i - b_{t+\eta}^{i,s}) q^2\left(\frac{\gamma_{t+\eta,1}^i - b_{t+\eta}^{i,s}}{\sigma_v}\right)}{Q\left(\frac{\gamma_{t+\eta,1}^i - b_{t+\eta}^{i,s}}{\sigma_v}\right) \left[1 - Q\left(\frac{\gamma_{t+\eta,1}^i - b_{t+\eta}^{i,s}}{\sigma_v}\right) \right]} \\ & + \sigma_v \sum_{r=1}^4 \sum_{s=1}^{N_s} \left[\frac{\partial h_{t+\eta}^i(\mathbf{x}_{t+\eta}^s)}{\partial \mathbf{x}_{t+\eta,r}} \right]^2 \frac{q^3\left(\frac{\gamma_{t+\eta,1}^i - b_{t+\eta}^{i,s}}{\sigma_v}\right) (2Q\left(\frac{\gamma_{t+\eta,1}^i - b_{t+\eta}^{i,s}}{\sigma_v}\right) - 1)}{Q^2\left(\frac{\gamma_{t+\eta,1}^i - b_{t+\eta}^{i,s}}{\sigma_v}\right) \left[1 - Q\left(\frac{\gamma_{t+\eta,1}^i - b_{t+\eta}^{i,s}}{\sigma_v}\right) \right]^2} \\ & = 0, \end{aligned}$$

where $\gamma_{t+\eta,1}^i$ represents the quantization threshold of the i th sensor at time $t + \eta$, $b_{t+\eta}^{i,s} \triangleq h_{t+\eta}^i(\mathbf{x}_{t+\eta}^s)$, and $h_{t+\eta}^i(\cdot)$ is the measurement model.

Proof: The result can be easily obtained by taking the first-order derivative of (16). ■

B. Identical Quantizers

It is clear from (14) that local quantizer design relies on the sensor location and the predicted measurement $h_{t+\eta}^i(\mathbf{x}_{t+\eta}^s)$, which theoretically verifies the statement in [4] that the use of identical quantizers at all the sensors leads to performance degradation. On the other hand, if we consider a linear measurement model $y_t^i = \mathbf{h}_t^i \mathbf{x}_t + v_t^i$ for sensor i at time t , where $\mathbf{h}_t^1 = \dots = \mathbf{h}_t^N$ (e.g., the mean estimation problem in [14]), it can be shown that the problem of quantizer design yields identical optimal thresholds for N sensors at every time instant due to the effect of identical sensor observation model on (5) and (12).

IV. SIMULATION RESULTS

In our simulations, we consider that $N = 9$ sensors are grid deployed in a 20×20 m^2 surveillance area. For target motion in (1), we select the sampling interval $\Delta = 0.5$ seconds and process noise parameter $q \in \{0.1, 2.5 \times 10^{-3}\}$, where the magnitude of q indicates the relative uncertainty regarding the target trajectory (see [1, Fig3] for an example). The initial state distribution of the target is assumed to be Gaussian with mean $\mu_0 = [-8.8, -8.8, 1.8, 1.8]$ and covariance $\Sigma_0 = \text{diag}[\sigma_0^2, \sigma_0^2, 0.01, 0.01]$ where $3\sigma_0 = 2$. We perform target tracking over 10 seconds, i.e., 20 time steps ($T_w \leq 20$). Sensor measurements are obtained from (3), where $P_0 = 1000$ and sensor observation noise with $\sigma_v = 0.1$. We assume that the fusion center has perfect information about the target dynamical model and the noise statistics. Observing from simulation results, which are omitted here for brevity, using 1000 and 50 particles in target estimation and quantizer design, respectively, provides a suitable tradeoff between the number of particles and tracking performance, which is evaluated in terms of mean square error (MSE) over 100 trials.

In Fig. 1, we demonstrate the tracking performance of the 2-bits non-myopic quantizer for different time window sizes, i.e., $T_w \in \{1, 5, 10, 20\}$, where the non-myopic design with $T_w = 1$ is equivalent to the myopic design, and the non-myopic quantizer with $T_w = 20$ becomes an offline quantizer since the corresponding A-CPCRLB is calculated offline. For comparison, we also present the tracking performance when using analog data (AD) and quantized data based on the offline Fisher information heuristic quantizer (FIHQ) [5]. As we can see, our proposed quantization strategy yields better performance than FIHQ. Specifically, Fig. 1-(a) shows that the estimation performance improves as T_w decreases. This is because for $q = 0.1$, the target trajectory has relatively large uncertainty so that the accuracy of estimation benefits from quantizer design using more sensor measurements. However, Fig. 1-(b) shows that the MSE for all values of T_w lies close

to each other since the target trajectory is almost deterministic (and thus predictable) as $q = 2.5 \times 10^{-3}$.

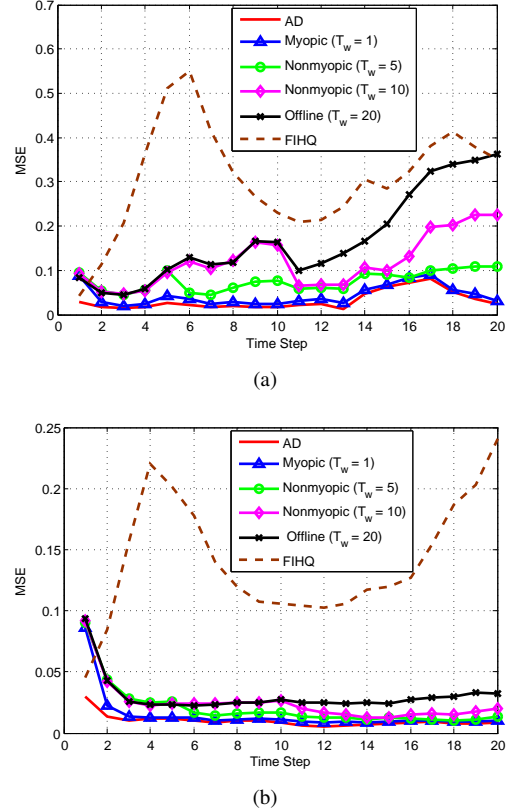


Fig. 1. Tracking performance of the non-myopic quantizer with different sizes of time window (a) $q = 0.1$ (b) $q = 2.5 \times 10^{-3}$

In Fig. 2, we present the MSE of temporally identical quantizer (I-Quantizer), which refers to the design of quantizers only for the next time step and then using the same quantizers over the entire time window. For comparison, the MSE of nonidentical quantizer (N-Quantizer) with $T_w = 20$ is also plotted. Simulation results show that the I-Quantizer yields worse performance than the N-Quantizer even with a small window size (i.e., $T_w = 2$). This is because in a tracking scenario the target state is random and dynamic, which leads to a large innovation error by using temporally-identical quantizers, although the identical design can save energy and computation cost.

V. CONCLUSION

In this paper, we considered the problem of target tracking with quantized data in a WSN, where the optimal local quantizers are determined using a non-myopic strategy. Using the alternative conditional posterior Cramér-Rao lower bound (A-CPCRLB) as the performance metric, we theoretically showed that the non-myopic quantizer can be designed separately for each time instant. With the help of a particle filtering method, this problem can be expressed in a closed form and solved via the interior-point algorithm. Simulation results demonstrated the effectiveness of our proposed approach. In

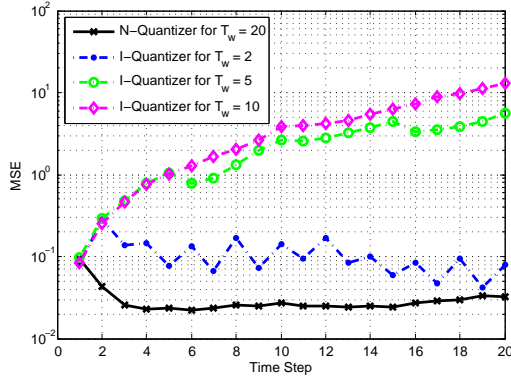


Fig. 2. MSE performances of 2-bits quantizer as $q = 2.5 \times 10^{-3}$

the future, we will consider the effect of channel statistics on quantizer design. We will also consider a unified non-myopic optimization framework for resource management problems such as sensor selection and bit allocation.

APPENDIX

Proof of Proposition 1: According to (7), problem (8) can be decomposed into two subproblems

$$\begin{aligned} & \underset{\gamma_{t+T_w}}{\text{maximize}} && E_{p_{t+T_w}^c} \left\{ -\nabla_{\mathbf{x}_{t+T_w}}^{\mathbf{x}_{t+T_w}} \ln p(\mathbf{u}_{t+T_w} | \mathbf{x}_{t+T_w}) \right\} \\ & \text{subject to} && \gamma_{t+T_w,1}^i < \dots < \gamma_{t+T_w,L-1}^i, \quad i = 1, \dots, N \end{aligned}$$

and

$$\begin{aligned} & \underset{\{\gamma_{t+\eta}\}}{\text{maximize}} && (Q + F J_{t+T_w-1}^{-1} F^T)^{-1} \\ & \text{subject to} && \gamma_{t+\eta,1}^i < \dots < \gamma_{t+\eta,L-1}^i \\ & && \eta = 1, \dots, T_w - 1 \text{ and } i = 1, \dots, N \end{aligned} \quad (17)$$

where Q and F are given by the process model (1).

Note that $Q + F J_{t+T_w-1}^{-1} F^T$ is positive definite since Q is positive definite and the information matrix J_{t+T_w-1} is positive definite (where we assume it is invertible). Then, problem (17) can be written as

$$\begin{aligned} & \underset{\{\gamma_{t+\eta}\}}{\text{minimize}} && Q + F J_{t+T_w-1}^{-1} F^T \\ & \text{subject to} && \gamma_{t+\eta,1}^i < \dots < \gamma_{t+\eta,L-1}^i \\ & && \eta = 1, \dots, T_w - 1 \text{ and } i = 1, \dots, N \end{aligned} \quad (18)$$

where we use the fact that, for any positive definite matrix, if $A \succeq B$ then $B^{-1} \succeq A^{-1}$.

Since F is invertible, the problem (18) is equivalent to

$$\begin{aligned} & \underset{\{\gamma_{t+\eta}\}}{\text{maximize}} && J_{t+T_w-1} \\ & \text{subject to} && \gamma_{t+\eta,1}^i < \dots < \gamma_{t+\eta,L-1}^i \\ & && \eta = 1, \dots, T_w - 1 \text{ and } i = 1, \dots, N \end{aligned}$$

Similarly, after T_w recursive decompositions, the problem (8) can be decomposed into T_w sub-problems given by

$$\begin{aligned} & \underset{\gamma_{t+\eta}}{\text{maximize}} && E_{p_{t+\eta}^c} \left\{ -\nabla_{\mathbf{x}_{t+\eta}}^{\mathbf{x}_{t+\eta}} \ln p(\mathbf{u}_{t+\eta} | \mathbf{x}_{t+\eta}) \right\} \\ & \text{subject to} && \gamma_{t+\eta,1}^i < \dots < \gamma_{t+\eta,L-1}^i, \quad i = 1, \dots, N \end{aligned} \quad (19)$$

Then by [8, Lemma 3.1], the problem (19) is equivalent to the problem (9), where for clarity, we reiterate the [8, Lemma 3.1] as below.

Consider two optimization problems

$$\max_{\mathbf{x} \in \mathcal{S}} M(\mathbf{x}) \quad (A_1)$$

$$\max_{\mathbf{x} \in \mathcal{S}} \text{tr}(M(\mathbf{x})) \quad (A_2)$$

where $M(\mathbf{x})$ is a matrix for an arbitrary $\mathbf{x} \in \mathcal{S}$, \mathcal{S} specifies the constraint on \mathbf{x} . If the problem (A_1) has an optimal solution, then the problem (A_1) is equivalent to (A_2) .

The proof of [8, Lemma 3.1] includes two parts. First it can be shown that if \mathbf{x}_1 is the optimal solution of (A_1) , then for arbitrary $\mathbf{x} \in \mathcal{S}$, $M(\mathbf{x}) \preceq M(\mathbf{x}_1)$ which yields $\text{tr}(M(\mathbf{x})) \leq \text{tr}(M(\mathbf{x}_1))$. Thus, \mathbf{x}_1 is also the optimal solution of (A_2) . On the other hand, if \mathbf{x}_2 is the optimal solution of (A_2) , then we have $\text{tr}(M(\mathbf{x}_1)) \leq \text{tr}(M(\mathbf{x}_2))$. Note \mathbf{x}_1 is the optimal solution of (A_1) which implies $\text{tr}(M(\mathbf{x}_2)) \leq \text{tr}(M(\mathbf{x}_1))$. Thus, we obtain $\text{tr}(M(\mathbf{x}_1) - M(\mathbf{x}_2)) = 0$. By $\text{tr}(M(\mathbf{x}_1) - M(\mathbf{x}_2)) = 0$ and $M(\mathbf{x}_1) - M(\mathbf{x}_2) \succeq 0$, we have $M(\mathbf{x}_1) = M(\mathbf{x}_2)$. Therefore, \mathbf{x}_2 is also the optimal solution of (A_1) . ■

ACKNOWLEDGMENT

This work was supported by U.S. Air Force Office of Scientific Research (AFOSR) under Grant FA9550-10-1-0263 and FA9550-10-1-0458.

REFERENCES

- [1] E. Masazade, R. Niu, and P. K. Varshney, "Dynamic bit allocation for object tracking in wireless sensor networks," *IEEE Trans. Signal Process.*, vol. 60, no. 10, pp. 5048–5063, Oct. 2012.
- [2] M. Vemula, M. F. Bugallo, and P. M. Djuric, "Particle filtering-based target tracking in binary sensor networks using adaptive thresholds," in *Proc. IEEE Int. Workshop on Comp. Advances in Multi-Sensor Adaptive Processing*, Dec. 2007, pp. 17–20.
- [3] M. Mansouri, O. Ilham, H. Snoussi, and C. Richard, "Adaptive quantized target tracking in wireless sensor networks," *Wireless Networks*, vol. 17, no. 7, pp. 1625–1639, Oct. 2011.
- [4] O. Ozdemir, R. Niu, and P. K. Varshney, "Adaptive local quantizer design for tracking in a wireless sensor network," in *Proc. the 42nd Asilomar Conf. Signals, Systems and Computers*, Oct. 2008, pp. 1202–1206.
- [5] R. Niu and P. K. Varshney, "Target location estimation in sensor networks with quantized data," *IEEE Trans. Signal Process.*, vol. 54, no. 12, pp. 4519–4528, Dec. 2006.
- [6] Y. Zheng, O. Ozdemir, R. Niu, and P. K. Varshney, "New conditional posterior Cramér-Rao lower bounds for nonlinear sequential Bayesian estimation," *IEEE Trans. Signal Process.*, vol. 60, no. 10, pp. 5549–5556, Oct. 2012.
- [7] S. Boyd and L. Vandenberghe, *Convex Optimization*, Cambridge University Press, Cambridge, 2004.
- [8] X. Shen and P. K. Varshney, "Sensor selection based on generalized information gain for target tracking in large sensor networks," Arxiv preprint <http://arxiv.org/abs/1302.1616>, 2013.
- [9] A. S. Chhetri, D. Morrell, and A. Papandreou-Suppappola, "Efficient search strategies for non-myopic sensor scheduling in target tracking," in *Proc. the 38th Asilomar Conf. Signals, Systems and Computers*, 2004, vol. 2, pp. 2106–2110.
- [10] E. Masazade, R. Niu, and P. K. Varshney, "An approximate dynamic programming based non-myopic sensor selection method for target tracking," in *Proc. the 46th Annual Conf. Information Sciences and Systems*, March 2012, pp. 1–6.
- [11] L. Zuo, R. Niu, and P. K. Varshney, "Conditional posterior Cramér-Rao lower bounds for nonlinear sequential Bayesian estimation," *IEEE Trans. Signal Process.*, vol. 59, no. 1, pp. 1–14, Jan. 2011.
- [12] M. S. Arulampalam, S. Maskell, N. Gordon, and T. Clapp, "A tutorial on particle filters for online nonlinear/non-Gaussian Bayesian tracking," *IEEE Trans. Signal Process.*, vol. 50, no. 2, pp. 174–188, Feb. 2002.
- [13] H. L. Van Trees and K. L. Bell, *Bayesian Bounds for Parameter Estimation and Nonlinear Filtering Tracking*, Wiley-IEEE press, 2007.

- [14] A. Vempaty, B. Chen, and P. K. Varshney, "Optimal quantizers for Bayesian distributed estimation," *Proc. IEEE Int. Conf. Acoustics, Speech and Signal Processing*, 2013.